Growth of improved ultra-thin pristine SnO_2 films by electric field modified spray pyrolysis and DC reactive sputtering techniques

Shikha, D. K. Pandya, S. C. Kashyap, and S. Chaudhary

Thin Film laboratory, Department of Physics,
Indian Institute of Technology Delhi, New Delhi, India
E-mail: dkpandya@physics.iitd.ac.in

ABSTRACT

The present paper reports on the deposition of high conductivity (10^2 $ohm^{-1}.cm^{-1}$) SnO_2 ultrathin films (less than 50 nm) by spray pyrolysis and pulsed dc magnetron reactive sputtering techniques in the presence of electric field. A comparative study has been carried out on the electrical, structural and optical properties of SnO_2 films deposited on a glass substrate with and without the presence of electric field. This is possibly the first such report of fabricating such high conductivity ultrathin films by spray pyrolysis. An evolution of crystallographic structure with increasing field is observed.

Keywords: ultrathin films spray pyrolysis, SnO_2, reactive sputtering, electric field.

1 INTRODUCTION

Device miniaturization and high density ICs demand high quality nanocrystalline transparent conducting oxide (TCO) films. These films show unique properties on the nanometre scale, and their extensive use in modern semiconductor device applications have prompted their widespread investigations [1, 2]. The physical properties of ultrathin films of these functional materials strongly depend on the crystallite size and structure/roughness of the interface. Pure SnO_2, an *n*-type semiconductor, also belongs to the class of TCOs. It has a rutile structure and a wide energy gap ~3.6 eV [3]. Owing to its outstanding electrical, optical, and electrochemical properties, SnO_2 is extensively used in many applications such as catalytic support material, transparent electrodes, touch screens, flat panel displays, solar cells, and gas sensors [4, 5, 6]. It has been reported that the electrical properties of the films strongly depend on the size, orientation, and shape of SnO_2 grains in films. Due to its potential applications in such devices that require films of thicknesses 1 – 50 nm, it is now important to have a re-look on the material properties through fundamental research [7], and hence calls for a systematic investigation on the microstructure, and interface of ultra-thin films and their effect on various physical properties. There are several techniques that can be employed for the fabrication of different oxide thin films including reactive sputtering [8], evaporation [9], chemical vapour deposition [9, 10], dip coating [11] and spray pyrolysis [12, 13, 14]. Unlike physical vapour deposition techniques which require vacuum of high order, spray pyrolysis is a simple and low cost deposition technique of preparing transparent and conducting oxide films of uniform thickness. We have initiated efforts to modify this simple technique for preparation of films < 50 nm thickness. In this paper we present some of our results on growth and properties of pristine ultrathin SnO_2 films, using electric field assisted spray pyrolysis and pulsed dc magnetron reactive sputtering techniques.

2 EXPERIMENTAL

2.1 Spray pyrolysis

A schematic diagram of the spray pyrolysis set up employed for the growth of pristine SnO_2 films is shown in figure 1. Undoped tin oxide films were fabricated on the glass substrates at a temperature of 450°C using 0.1M solution of $SnCl_4.5H_2O$ in absolute ethanol. The flow rate (5 ml/min) of solution was controlled by a carrier gas at a pressure of 0·5 kg/cm^2. The nozzle was at a distance of 24 cm from the substrate during deposition. A potential difference of 32V was applied on the substrate during deposition.

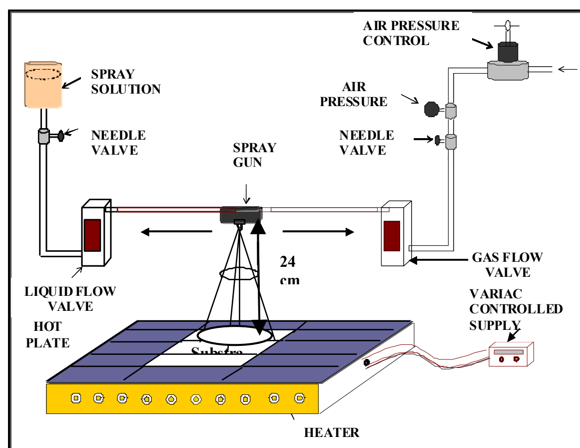

Fig. 1 Schematic diagram of the Spray pyrolysis system

2.2 DC Magnetron Reactive Sputtering

Tin oxide films were also prepared by pulsed dc magnetron reactive sputtering technique. The target was a metallic disk of Sn (purity 99.9%). The target–substrate distance was 10 cm. A thermocouple was positioned on the reverse side of the substrate holder to control the substrate temperature during the film growth, the sputtering gases were O_2 and Ar, which were combined in the sputtering chamber. Before deposition, the sputtering chamber was pumped down to 8×10^{-6} Torr. The target was pre-sputtered in O_2 for 15 min, in combination with a shutter, ensuring stabilized sputtering conditions. Total sputtering pressure of $2.2\text{x}10^{-2}$ Torr was used. The Ar flow rate was 15 sccm and oxygen flow rate was maintained at 3.5 sccm. During deposition the substrate temperature was 350°C and the deposition rate was 1.5nm/min.

The film thickness was measured using XRR and ellipsometry. Optical transmission studies of all the films prepared by both the methods were made using a UV-VIS IR double beam spectrophotometer. The crystallographic structure of the films was studied by by X'PertPRO X-ray diffraction system using CuKα radiation. The electrical properties were studied by Van der Pauw method.

3 RESULTS AND DISCUSSION

3.1 Structural Analysis

The XRD patterns obtained for the films grown on glass substrates were studied in the 2θ range of 20°-80°. The XRD patterns (Fig. 2) show that the SnO_2 films are polycrystalline in nature irrespective of the technique used for deposition. The matching of the observed and the standard d-values from JCPDS data PDF #770449 confirms that the deposited films are of SnO_2 with tetragonal structure. All the patterns contain the characteristic SnO_2 peaks only. The presence of other phases such as SnO, Sn_2O_3 is not found in the present study. The pristine films grown by both the techniques are therefore single phase. The lattice constant 'a' and 'c', for the tetragonal phase structure is determined by the relation

$$\frac{1}{d^2} = \left(\frac{h^2 + k^2}{a^2}\right) + \left(\frac{l^2}{c^2}\right) \qquad (1)$$

where 'd' is the interplaner distance and (hkl) are miller indices, respectively. The calculated average lattice parameter values are a = 4.7 Å and c = 3.2 Å.

The lattice parameter values are in good agreement with the standard data. The average grain size of the SnO2 thin films was calculated by using Scherer's formula [8].

$$D(nm) = \left(\frac{0.9\lambda}{\beta \cos\theta}\right) \qquad (2)$$

'λ' is wavelength of X-ray, 'β' is the full-width at half of the peak maximum in radians and 'θ' is Bragg's angle. The grain size of these samples is given in Table 1.

Table 1

Deposition Technique	Thickness (nm)	Grain size (nm)
Spray Pyrolysis Without Electric Field	30	24.5
Spray Pyrolysis With Electric Field of 32V/cm	30	18.6
Pulsed DC magnetron reactive sputtering without Electric Field	30	19.9

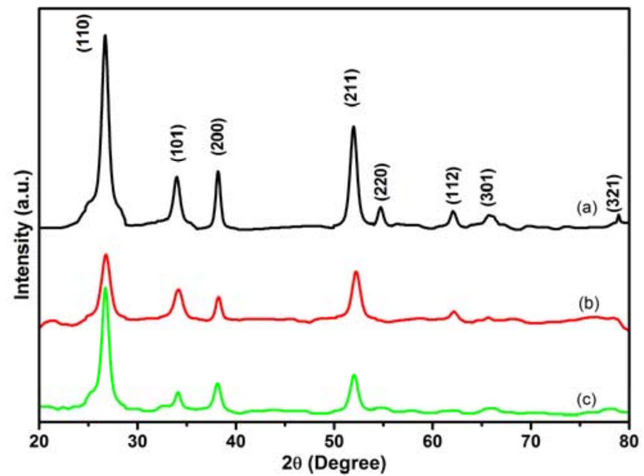

Fig.2. XRD pattern of SnO_2 films of thickness 30nm deposited by spray pyrolysis by applying (a) zero electric field and (b) 32V/cm electric field at the substrate during deposition, and (c) by pulsed dc magnetron reactive sputtering technique at zero electric field.

Table 2

Applied Electric Field (V/cm)	Grain size (nm)
0	19.9
14	20.2
32	21.3

Figure 3 shows the XRD pattern of ultrathin films deposited by pulsed dc magnetron reactive sputtering at different field values showing a trend of systematic prominence of (110) peak at the expense of (200) peak. Futher study is in progress for a clear picture. The variation of the grain size with applied electric field is given in Table 2.

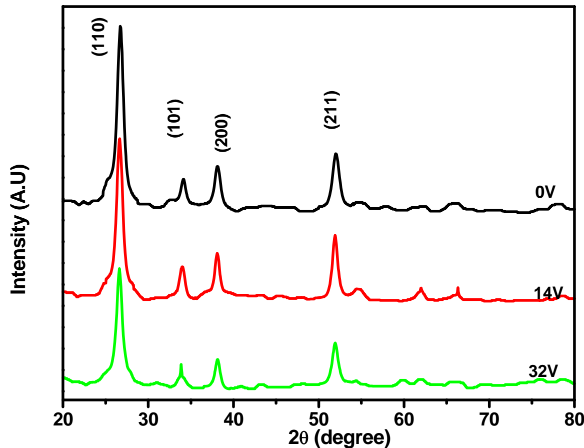

Fig.3. XRD pattern of SnO_2 films of thickness 30nm deposited by pulsed dc magnetron reactive sputtering technique by applying different electric field

3.2 Electrical Properties

The values of Hall mobility, carrier density and resistivity measured at room temperature are shown in Table 3. The values of μ, *n* and ρ for SnO_2 films deposited by different techniques are obtained from the combined measurements of resistivity and Hall coefficient. The electrical conductivity is increased by one order i.e. from 3.8 to 14.7ohm^{-1}cm^{-1}, SnO_2 films when films are deposited under electric field by spray pyrolysis technique. It is also found that the films deposited by sputtering technique are more conducting than the films deposited by spray pyrolysis. The decrease in the resistivity can be explained on the basis of the observed increase in the carrier concentration, from 7.04x10^{17} to 7.24x10^{18} cm^{-3}, for the film deposited by spray pyrolysis in the presence of electric field.

Table 3

Deposition Technique	**T_s (°K)**	**R_s (Kohm / sq)**	**N (per cc)**	**μ (cm^2/ V. s)**	**ρ (Ω cm)**
Spray Pyrolysis Without Electric Field	450	88.40	7.04x 10^{17}	25.49	2.6x 10^{-1}
Spray Pyrolysis With Electric Field of 32V/cm	450	22.75	7.24x 10^{18}	9.6	6.8x 10^{-2}
Pulsed DC magnetron reactive sputtering	350	10.19	2.38x 10^{19}	8.58	3.0x 10^{-2}

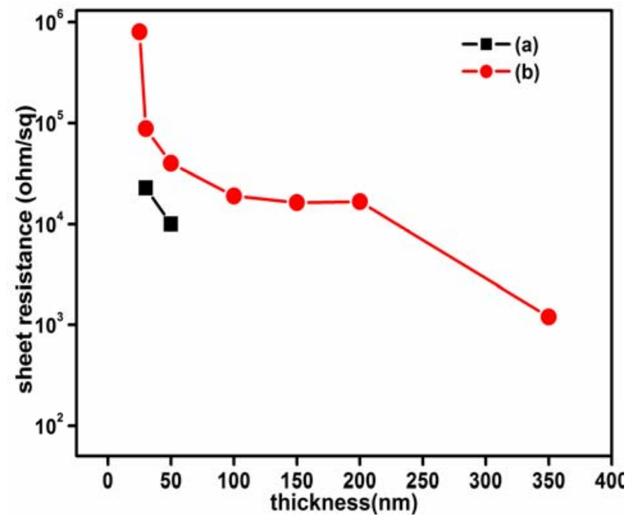

Fig.4. Sheet resistance vs. thickness plot for the spray pyrolysed SnO_2 films (a) with and (b) without electric field.

Figure 4 shows the variation of sheet resistance with the film thickness of the SnO_2 films deposited by spray pyrolysis without electric field and in the presence of electric field (32V/cm). We can observe () that for a film of thickness 30 nm the sheet resistance drops by about a factor of 40 if field is applied during deposition.

3.3 Optical properties

Figure 5 shows the transmission spectra of our spray pyrolysed and sputtered films. The films by spray pyrolysis are highly transparent (90%) in the visible region. However, films deposited at 350°C by sputtering are found to be some what less transparent in this region.

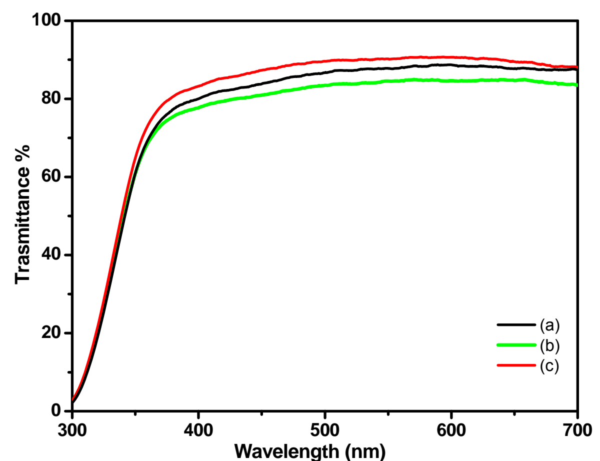

Fig.5 Optical transmittance spectra of SnO_2 films (a) sputtered without electric field, (b) spray pyrolysed without electric field and (c) spray pyrolysed with field of 32V/cm.

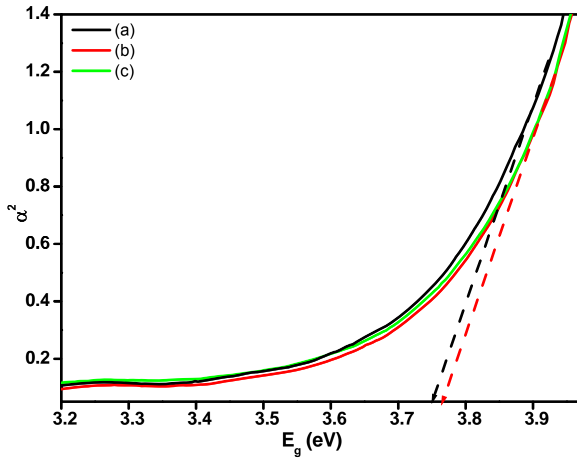

Fig.6. Plot of α^2 vs E_g of SnO_2 film (a) sputtered without electric field, (b) spray pyrolysed without electric field and (c) spray pyrolysed with field of 32V/cm.

From the transmission spectra, optical parameters like absorption coefficient (α), and optical band gap, E_g have been calculated. The absorption coefficient (α), have been determined by using the relation:

$$\alpha = \frac{\ln((1-R)/T)}{d} \quad (3)$$

where d is the thickness of the film in cm, T and R are the transmittance and reflectance of the film. The optical band gap energy of SnO_2 film was determined using the equation

$$\alpha h\nu = A(h\nu - E_g)^{1/2} \quad (4)$$

where A is a constant. To calculate the optical energy band gap value for a particular film α^2 vs. energy graph is plotted, as in figure 6, and by extrapolating the straight line, the intercept on the energy axis at $\alpha = 0$ is determined. The optical energy band gap is found to be nearly 3.75 eV.

4 CONCLUSIONS

Highly conducting and transparent ultrathin pristine SnO_2 films were fabricated on glass by electric field modified spray pyrolysis and DC reactive sputtering techniques. SnO_2 films grown by both the techniques were transparent in visible region with transparency of about 90% and band gap was found to be 3.75eV. The electrical conductivity of the films of 30 nm thickness was enhanced by more than one order i.e. from 3.8 to 14.7ohm^{-1}cm^{-1} when deposited in the presence of electric field which is interpreted in terms of an increase the carrier density. So we can conclude that the electric field plays a pivotal role in controlling the physical properties of ultrathin films.

REFERENCES

[1]. H. L. Tuller, J. Electroceram. 1, 1997, 211.
[2]. H. Gleiter, Acta Mater. 1, 2000, 48.
[3]. J. Robertson, Phys. Rev. B 30, 1984, 3520.
[4]. N. Romeo, A. Bosio, R. Tedeschi, A. Romeo and V. Canevari, Solar Energy Mat. & Solar Cells, 58, 1999, 200.
[5]. Y. Fukuma, F. Odawara, H. Asada and T. Koyanagi, Phy. Rev. B 78, 2008, 104417.
[6]. T. Minami, Semicond. Sci. Technol. 20, 2005, S35.
[7]. K. L. Chopra, S. Major, D. K. Pandya, Thin Solid Films, 102, 1983, 1
[8]. B.D. Cullity, Elements of X-Ray Diffraction, A. W. Pub. Comp. Inc., 1978, 99.
[9]. S.S. Pan, C. Ye, X.M. Teng, H.T. Fan, G.H. Li, Appl. Phys. A 85, 2006, 21.
[10]. J. Sundqvist, A. Harsta, in Proceedings of the Sixteenth International CVD Conference, 1, Paris, France, 2003, 511.
[11]. V. Geraldo, Luis Vicente De Andrade Scalvi, Evandro Augusto De Morais, Celso Valentim Santilli, Sandra Helena Pulcinelli, Mater. Res. 6, 2003, 451.
[12]. S. Chaudhary, K. P. Bhatti, D. K. Pandya, and S. C. Kashyap and A.K.Nigam, J Mag Mag Mat, 321, 2009, 966.
[13]. S. C. Kashyap, K. Gopinadhan, D. K. Pandya and S. Chaudhary, J Mag Mag Mat, 321, 2009, 957.
[14]. Archana Gupta, Dinesh K. Pandya and Subhash C. Kashyap, Jap. J. of Appl. Phys. 43, L 1592, 2004.